Pathol. Oncol. Res. (2016) 22:421–430
DOI 10.1007/s12253-015-0025-6

ORIGINAL ARTICLE

Isolation and Characterization of a Murine Spontaneous High-Grade Follicular Lymphoma with Restricted In Vivo Spreading – a Model for Lymphatic Metastasis Via the Mesentery

Dóra Vojkovics[1,2] · Zoltán Kellermayer[1,2] · Diána Heidt[1,2] · Martina Mihalj[3] · Béla Kajtár[4] · Dávid Ernszt[5] · Tamás Kovács[5] · Péter Németh[1] · Péter Balogh[1,2]

Received: 12 July 2015 / Accepted: 16 November 2015 / Published online: 19 November 2015

Abstract Spontaneous or induced malignant lymphomas in mice are valuable tools for studying human lymphoproliferative diseases, including the mechanism of migration between peripheral lymphoid organs and positioning within distinct tissue compartments. Here we report the isolation and characterization of a novel spontaneous lymphoma from BALB/c mice showing restricted tissue distribution and metastasis. The lymphoma cells display CD19, B220, MHC II, surface IgG2a/kappa chain with V_H7183 rearrangement of the *IgH* gene, indicating their B-cell origin. Serial intraperitoneal injection of primary tumor into both BALB/c and RAG-1-deficient hosts led to the successful propagation of lymphoma. Despite the cytological characteristics of high-grade follicular B-cell lymphoma, the tumor cells (denoted as Bc-DLFL.1) showed significantly lesser spreading to extraabdominal locations upon intraperitoneal passage compared to splenic and mesenteric lymph node expansion. In mesenteric lymph nodes the high endothelial venules contained only few tumor cells, while the lymphatic vessels were almost completely filled with lymphoma cells. Similarly, the LYVE-1-positive lymphatic capillaries within the mesentery were packed with lymphoma cells. These findings suggest that Bc-DLFL.1 cells likely propagate primarily via the lymphatic circulation within the mesentery, therefore this tumor may offer an *in vivo* model to investigate the tumor cell migration via the lymphatic circulation from the peritoneal cavity.

Keywords Mouse · Follicular lymphoma · Lymphatics · Model

✉ Péter Balogh
balogh.peter@pte.hu

[1] Department of Immunology and Biotechnology, University of Pécs, Szigeti út 12, Pécs H-7624, Hungary

[2] Lymphoid Organogenesis Research Group, Szentágothai Research Center, University of Pécs, Pécs, Hungary

[3] Department of Physiology and Immunology, School of Medicine Josip Juraj Strossmayer University of Osijek, Osijek, Croatia

[4] Department of Pathology, University of Pécs, Pécs, Hungary

[5] Department of Pharmaceutical Biotechnology, University of Pécs, Pécs, Hungary

Introduction

Maturation of resting B lymphocytes following antigen stimulation into plasma cells or memory B cells in peripheral lymphoid tissues is a multistep process requiring a tightly regulated sequence of activation, proliferation and clonal selection. In this process uncontrolled expression of a limited number of crucial genes leads to various forms of differentiation blockade, causing abnormal proliferation or survival of transformed B cells. Depending on the phenotypic and genotypic traits, the resulting B-cell malignancies have broadly variable differentiation stages of affected cells, cellular composition and lymphoid and other tissue involvement [1, 2].

For the more efficient diagnosis and therapy of human B-cell lymphomas, various spontaneous B-cell tumors in mice have proved invaluable tools. Earlier these tumors arose either spontaneously or were induced by ionizing irradiation, exposure to chemical agents or viral transformation [3]. Subsequent identification of certain key elements (such as c-myc and Bcl-2) involved in the malignant transformation of B cells in humans combined with the ability to manipulate the mouse genome has greatly expanded the potential research models [4, 5], but also raised the importance of species differences, as various murine models were often found to be different from the parallel human conditions, including both the

phenotypic characteristics of malignant cells and the course of the disease [5, 6]. This divergence may reflect important structural differences between the human and mouse lymphoid organs themselves (such as the composition of splenic marginal zone and Peyer's patches, [7]) or the divergent expression pattern of cell surface markers used for the identification of various B-cell subsets [2].

In addition to providing potential in vivo models for human diseases, murine B cell lymphomas may also offer experimental opportunities to study the mechanisms of interactions between the lymphoid and non-hematopoietic constituents in peripheral lymphoid tissues. These include the preserved capacity of lymphoma cells to selectively colonize peripheral lymphoid tissues via organ-selective homing and subsequent positioning within suitable microenvironmental niches, as an analogue to the lymphocyte compartmentalization under physiological conditions, including their capacity to modulate their stromal milieu [8, 9].

In this paper we report the isolation and characterization of a BALB/c mouse-derived novel spontaneous B-cell lymphoma. We demonstrate that the intraperitoneal injection of this lymphoma results in a selective tumor seeding of the spleen and mesenteric lymph node, where the metastasis is formed via the lymphatic vasculature of mesentery. Thus this novel B-cell lymphoma may offer a unique model for studying the in vivo lymphatic propagation of B-cell tumors.

Materials and Methods

Mice

Inbred BALB/c and *Rag1*$^{-/-}$ [10] mice were originally purchased from Jackson Laboratory, and were maintained under SPF conditions at the Department of Immunology and Biotechnology under permits BAI/01/1390–003/2013 (issued by the Baranya County Government Office) and SF/688–18/2013 and SF/27–1/2014 (issued by the Ministry of Agriculture). After their retrieval from the SPF unit the mice were kept under clean conditions with 12 h of light/dark cycles and were provided with water and pelleted food *ad libitum*.

Lymphoma Cell Isolation and Passage

The original tumor was mechanically dispersed using a 70 μm cell strainer (BD Biosciences, Soft Flow Ltd., Pécs, Hungary) and resuspended in DMEM medium (Sigma-Aldrich, Budapest). The tumor cells at the dose of 10^7 cells/recipients in 0.2 ml medium were injected intraperitoneally. For tumorigenicity testing various doses of lymphoma cells were injected intraperitoneally and the mice were observed daily up to 30 days. Mice with terminal stage tumor were sacrificed by cervical dislocation, and their lymphoid and other organs were collected under aseptic conditions in a laminar flow. For further passage mesenteric lymph node (mLN) and spleen were collected and processed by mechanical dispersion through 70 μm mesh size cell strainer (BD Biosciences, Soft Flow Hungary, Pecs).

Antibodies and Reagents

Rat mAb against MHC Class II (IBL-5/22) was produced in our lab [11] and was used as hybridoma supernatant. mAb against peripheral lymph node addressin (PNAd, clone MECA-79) was purchased from BD Biosciences (Soft Flow Hungary, Pecs), anti-LYVE-1 (clone 223,322) and goat anti-mouse Bcl-6 antibodies from R&D Systems (Biomedica Hungária Kft, Budapest). Anti-mouse VEGF-R2/flk-1 mAb (clone Avas12α1) was purchased from BD Biosciences. Anti-mouse CD19 (clone B3B4), anti-mouse CD3 (clone KT-3), anti-mouse LFA-1 (clone M14.4) and anti-mouse L-selectin/CD62L (clone MEL-14) and anti-mouse ICAM-1/CD54 (clone YN1/1) hybridoma lines were obtained from ATCC, anti-α4 integrin mAb (from clone PS/2) was kindly provided by Dr. Eugene C. Butcher. Anti-B220 IgG (clone RA3-6B2 from ATCC) was purified by Protein G chromatography and labeled with FITC or Alexa Fluor 568 dye (Life Technologies Magyarország Kft, Budapest) using standard labeling conditions or used as hybridoma supernatant. FITC-conjugated anti-mouse IgM, IgG1, IgG2a, IgG2b and IgA rabbit antibodies were purchased from Sigma-Aldrich. Control rat IgG was purified from Wistar rat serum using Protein G affinity chromatography. The unlabeled rat mAbs and the goat polyclonal antibodies were detected with goat anti-rat IgG or donkey anti-goat IgG respectively, conjugated with FITC or PE (BD Biosciences). For immunohistochemical staining the anti-B220 mAb was detected by Histols polymeric anti-rat IgG HRPO-conjugate (Hisztopatologia Kft, Pécs, Hungary).

Flow Cytometry

Single cell suspension prepared from mLN, peripheral lymph nodes (pLN) or spleen of *Rag1*$^{-/-}$ or BALB/c recipients were incubated with monoclonal antibodies against MHC Class II, CD3, CD19, B220 or normal rat IgG and various anti-mouse immunoglobulin isotype antibodies at 10 μg/ml in PBS containing 0,1 % Na-azide and BSA for 30 min followed by two washing steps. The bound antibodies were detected using FITC-conjugated goat anti-rat IgG, followed by washing. The cells were fixed in 1 % buffered paraformaldehyde and the samples were analyzed using a Becton-Dickinson FACSCalibur and the CellQuest Pro software. Typically ten thousand single lymphocyte events as defined by their FSC/SSC characteristics were collected.

Histology and Immunohistology

Formol-fixed and paraffin embedded tissues (spleen, mesenteric lymph nodes and mesenterium, thymus, peripheral lymph nodes, liver, kidney, lungs and brain) were processed according to standard histological procedures using hematoxylin-eosin and periodic acid-Schiff staining. For immunohistochemical or immunofluorescent labeling tissues were placed in Killik embedding medium and snap-frozen in plastic molds. Frozen sections at 8 μm thickness were cut with a Leica cryostat and placed onto microscopic slides, and were allowed to dry. After fixing in cold acetone the sections were allowed to dry. The endogenous peroxidase activity was quenched with 0,1 % phenyl-hydrazine hydrochloride in PBS for 20 min followed by washing. After blocking with 5 % BSA in PBS for 20 min anti-B220 antibody was added and incubated for 45 min. After washing polymeric Histols anti-rat IgG-HRPO conjugate was added and incubated for 45 min. After repeated washing the enzymatic reaction was developed using DAKO acetate buffer and diamino-benzidine solution, and mounted using Permount medium.

For dual immunofluorescence after fixation in acetone the slides were allowed to dry, and then rehydrated in 5%BSA-PBS. Next the sections were incubated either with anti-LYVE-1 or anti-PNAd mAbs, followed by FITC-conjugated goat anti-rat IgG. After washing the residual binding sites of the secondary antibody were saturated with normal rat serum at 1:50 dilution for 20 min, followed by adding Cy3-conjugated anti-B220 mAb. After incubation the sections were repeatedly washed in PBS and covered in 1:1 PBS-glycerol, and viewed under Olympus BX61 fluorescent microscope.

Analysis of IgH Rearrangement

DNA from $2x10^5$ lymphoma cells was extracted using Qiagen QIAamp DNA Micro Kit according to the user's instructions. The rearrangement status of Ig heavy chain gene was determined by PCR reaction using degenerate primers for various murine V_H families as described [11]. The amplified products were electrophoresed and visualized using Biotium GelRed. The images were recorded using Bio-Rad Gel Doc XR instrument and Image Lab 5.0.0 software.

Statistical Analysis

Survival data for Kaplan-Meier evaluation were statistically analyzed by logrank (Mantel-Cox) test using GraphPad Prism software.

Results

Identification of a Spontaneous High-Grade B-Cell Follicular Lymphoma

As an incidental finding during the dissection of an aged BALB/c female mouse a soft tissue mass was found surrounding the terminal segment of ileum, accompanied with a robust splenomegaly. Macroscopic observation of the abdominal organs, lungs and brain and also peripheral lymph nodes (inguinal, cervical and brachial) and Peyer's patches did not reveal any gross pathology. To test whether the splenic enlargement may be caused by lymphohematopoietic malignancy the enlarged spleen was removed and single cell suspension was injected intraperitoneally into a cohort of BALB/c recipients. The injected mice showed a sharp decline of physical activities at around 15–18 days after the injection, and after sacrificing the moribund mice we observed enlarged mesenteric lymph nodes (mLN) and spleen, similar to the original tumor-bearing mouse (Fig. 1a). The tumors were removed and processed for serial *in vivo* passage as well as cryopreservation. Histological sections prepared from the mLN and spleen showed a vaguely nodular lymphoid infiltrate composed of centroblast and centrocyte-like atypical cells showing brisk mitotic activity. The ratio of centroblast-like cells was heterogeneous, on average approximately 40 %. The infiltrate replaced the follicles and extended in other lymphoid regions (Fig. 1 b, c and d). PAS staining revealed no positive labeling for the lymphoma cells (not shown).

In both syngeneic BALB/c and allogeneic *Rag1*$^{-/-}$ recipients the tumor cells could efficiently be propagated. We found that injecting large number of cells ($2.5x10^7$ and $2.5x10^6$ cells in each recipient) could uniformly lead to death within 15 days ($p < 0.001$), and even $2.5x10^5$ cells/recipient were sufficient to induce 50 % mortality in BALB/c recipients (Fig. 2) within 30 days ($p < 0.01$).

Given the relative frequent appearance of B-cell derived malignancies in aged BALB/c mice [12], to define the hematopoietic lineage affiliation of the tumor we performed immunohistochemistry using B220 as a B-cell antigen. We found that both the splenic white pulp and the mLN contained homogenously B220-positive lymphoma cells, although at some locations within the splenic white pulp some remnants of the original follicles could be found, based on their more intense B220 expression (Fig. 3a, b). To further verify the B-cell origin of this spontaneous lymphoma we performed flow cytometric phenotyping using CD19 and MHC Class II labeling, using B220 as reference marker in tumor cell suspension obtained from *Rag1*$^{-/-}$ recipients. To rule out T-cell malignancy we also labeled the cells for CD3 and CD5. Positive reactivity for CD19, MHC class II, in addition to B220 and the lack of CD3 expression and CD5 production (not shown) confirmed our earlier immunohistochemical results for B220

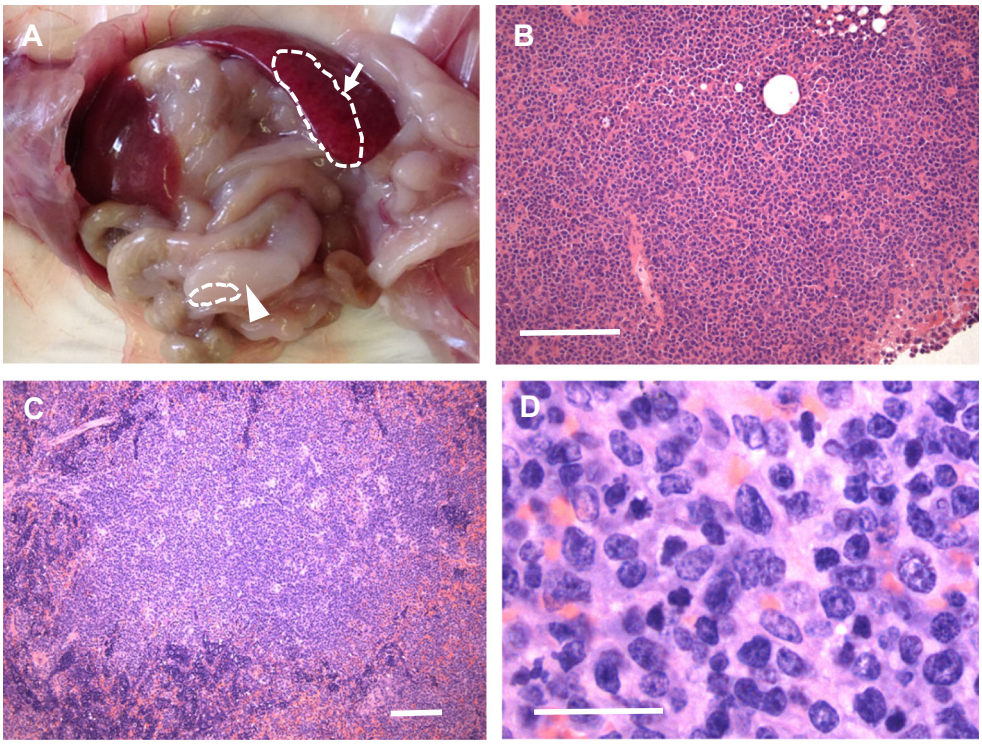

Fig. 1 Macroscopic appearance and histopathology of Bc-DLFL.1 lymphoma. Macroscopic pathology **a** reveals significant splenomegaly (*arrow*) and enlarged mLNs (*arrowhead*), with the dotted lines outlining the borders of organs in control mice. H&E staining of mLN (**b**; scale bar = 200 μm) and spleen (**c**; scale bar = 200 μm) shows lymphoma infiltrate composed of centroblasts intermingled with centrocytes in a representative spleen sample from a BALB/c recipient injected with lymphoma cells (**d**; scale bar = 20 μm)

expression, thus establishing the B-cell origin of this lymphoma (Fig. 3c). Taken together the B-lineage surface markers with the cytological characteristics, this lymphoma corresponds to follicular lymphoma of mixed cell type according to the Bethesda proposal for classification of lymphomas in mice, an entity similar to the high-grade variant of follicular lymphoma category in humans. Correspondingly we denote this tumor as Bc-DLFL.1 (BALB/c-derived Diffuse Large cell Follicular Lymphoma.1).

Immunoglobulin Gene Expression and Production in the Bc-DLFL.1 Lymphoma

Most B-cell lymphomas in both humans and mice express productively rearranged immunoglobulin genes. To test whether such a rearrangement results in detectable cell surface immunoglobulin, we stained the lymphoma cells for IgM, IgD, IgG

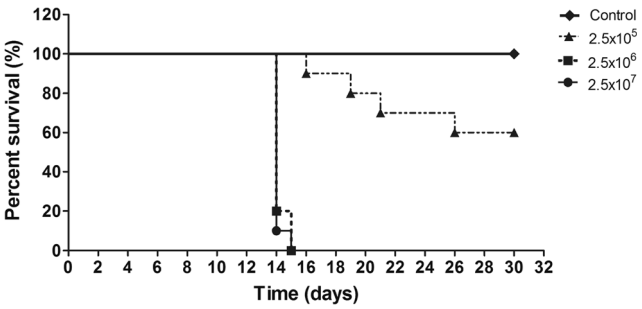

Fig. 2 Dose-dependence of lymphoma engraftment and mortality. Survival of a cohort of BALB/c mice ($n = 10$ recipients/group) following intraperitoneal injection of lymphoma cells at various doses

subclasses and IgA, in addition to kappa light chain. We found positive reactivity for kappa chain and IgG2a without the appearance of IgM, IgD, other IgG classes or IgA (Fig. 4a).

To determine the rearrangement pattern of the Ig heavy chain gene variable region of the Bc-DLFL.1 lymphoma we amplified the genomic DNA using V_H-family specific primer pairs. We found rearrangement of IgH genes within the V_H7183 region in lymphoma cells isolated from both BALB/c and *Rag1*$^{-/-}$ recipients using normal BALB/c mLN as reference sample for successful IgH V-region amplification (Fig. 4b).

The presence of IgG2a/κ surface immunoglobulin indicated isotype switch, usually associated with B cells having undergone germinal center (GC) reaction coupled with Ig affinity maturation, in which process Bcl-6 transcriptional repressor plays a crucial role [13, 14]. As GC-derived B-cell lymphomas in humans overwhelmingly express of Bcl-6, next we investigated the presence of Bcl-6 in Bc-DLFL.1 by flow cytometry. We found Bcl-6 expression in the majority of lymphoma cells, thus further confirming the GC origin of the Bc-DLFL.1 lymphoma (Fig. 4c).

Analysis of Homing Receptor Expression in Bc-DLFL.1 Lymphoma

During the serial intraperitoneal passage of lymphoma cells we noted a robust early enlargement of the mesenteric lymph nodes (mLN) over the largely preserved size and structure of peripheral lymph nodes (pLN), which prompted us to analyze the cell surface adhesion molecules involved in leukocyte homing. We labeled freshly removed lymphoma cell

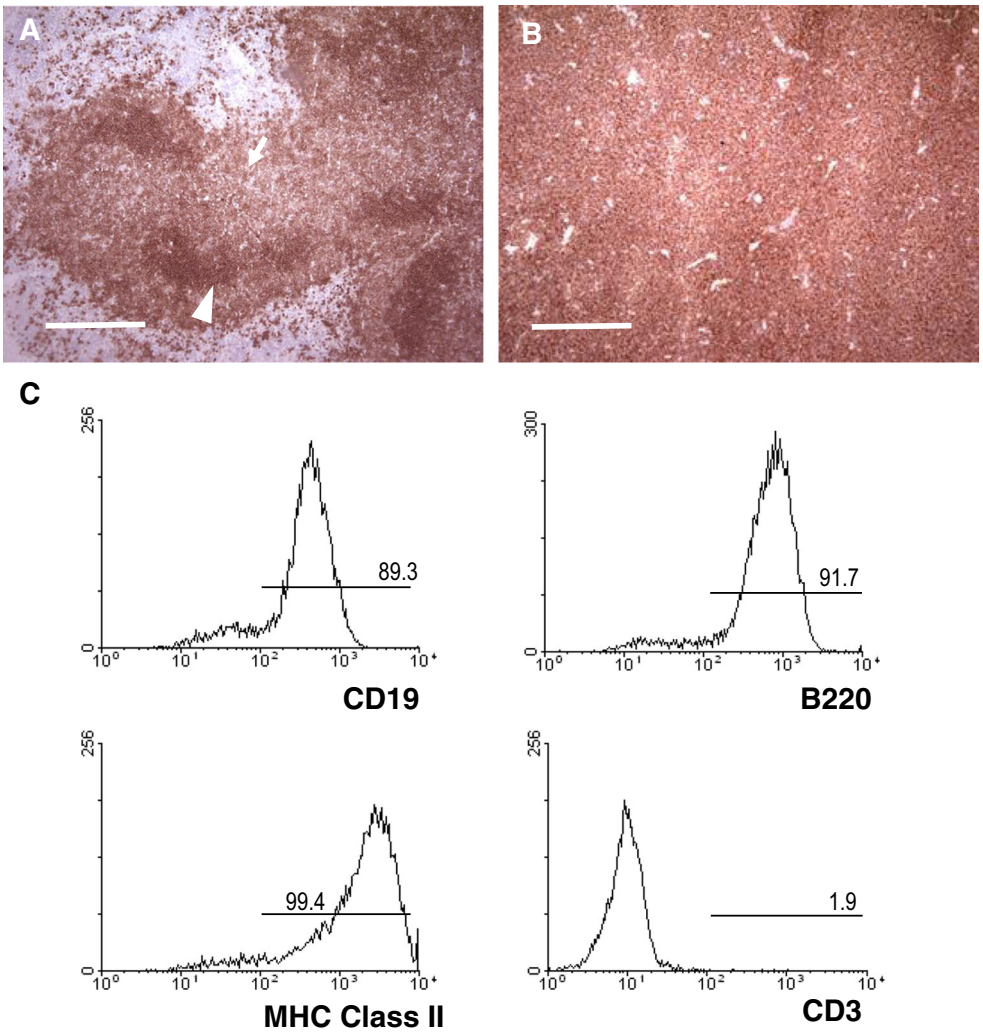

Fig. 3 Immunohistology and cell surface phenotype of Bc-DLFL.1 lymphoma. Anti-B220 staining of a spleen **a** and mLN **b** section from a lymphoma-injected BALB/c mouse reveals a homogenous infiltrate composed of $B220^{+}$ cells, where in the spleen both the remnants of follicles with more intense B220 expression (*arrowhead*) and lymphoma (*arrow*) with a weaker B220 display can be identified (a representative sample from a group of $n = 8$; scale bar = 200 μm). **c** A representative flow cytometric staining of lymphoma cells from the mLN a $Rag1^{-/-}$ recipient indicates the expression of B-lineage associated markers and lack of CD3 ($n = 7$). Numbers in the histograms correspond to the cumulative percentage of positive cells in the fluorescence channel range indicated by the horizontal line

suspension from mLN of $Rag1^{-/-}$ recipients with rat mAbs against LFA-1 (CD11α/CD18), ICAM-1 (CD54), L-selectin (CD62L) and α4 integrin. We found that all four adhesion receptors were produced and displayed on the cell surface, although at different degrees of expression. According to our findings, the lymphoma cells expressed ICAM-1 and LFA-1 molecules at a higher level compared to L-selectin and α4 integrin (Fig. 5).

Metastasis of Bc-DLFL.1 Lymphoma Cells to Mesenteric Lymph Nodes Involves Afferent Lymphatic Vessels of the Mesentery

In addition to the enlarged spleen and mLN in lymphoma-bearing mice, we also noticed a substantial swelling of perivascular adipose cuffs surrounding the arterioles in the mesentery, a bi-layered sheet of mesothelium. HE staining combined with immunohistochemical labeling for B220 revealed that lymphoma cells accumulate both in the reticular perivascular connective tissue and in tight compact clusters in luminal arrangement (Fig. 6a, b and c). This latter arrangement of lymphoma cells in thin-walled dilated lumens raised that lymphatic vessels connecting the intestines and mesenteric lymph nodes could be involved in the expansion of tumor. To confirm the lymphatic identity of these vessels tissue sections from mesentery and mesenteric lymph nodes were reacted with anti-LYVE-1 mAb against lymphatic endothelium and also against VEGF-R2/flk-1 as blood endothelium marker or PNAd as high endothelial cell marker, respectively, in combination with anti-B220 labeling. We found that B220-positive cells were tightly packed within LYVE-1 positive lymphatic vessels in both the mesentery and in the entire lymphatic vasculature of the mesenteric lymph node. In contrast, the blood vasculature (including the PNAd-positive high endothelial venules) of mLNs only rarely contained B220-positive lymphoblasts (Fig. 6d, e and f). From these observations we conclude that the primary dissemination pathway of Bc-DLFL.1 cells from the abdominal cavity towards the mLNs involves the lymphatic vessels connecting the intestines and mLNs.

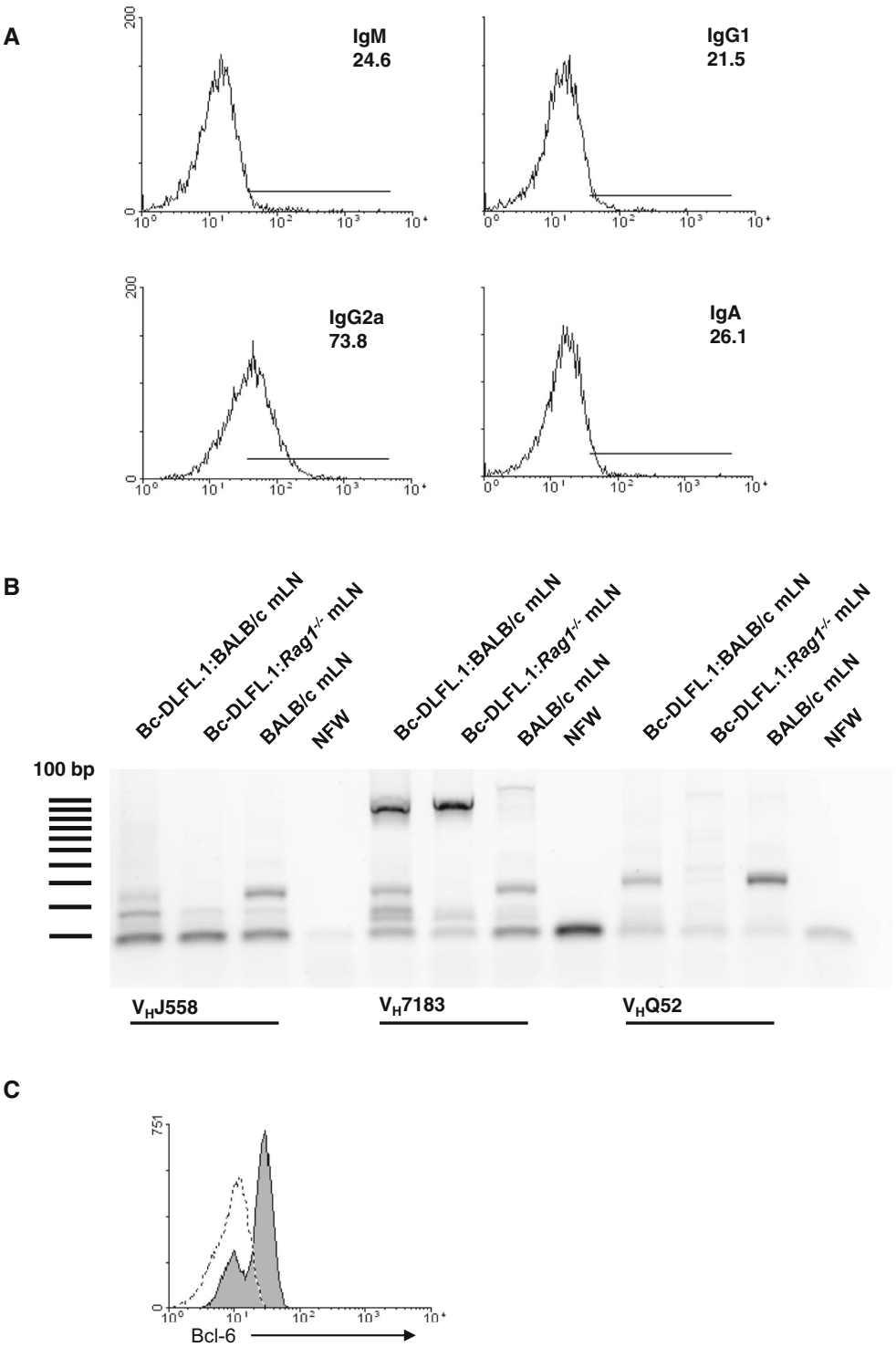

Fig. 4 BcR isotype and IgH V-rearrangement in Bc-DLFL.1 lymphoma. **a** B220-positive cells in *Rag1*$^{-/-}$ recipient mLN sample were stained for cell surface Ig isotypes as indicated, with the mean fluorescence intensities (MFI) shown ($n = 5$), where only IgG2a Ig subclass expression is detectable. **b** PCR analysis of IgH V-region rearrangement demonstrates identical VDJ-rearrangement of V_H7183 family in lymphoma-injected BALB/c or *Rag1*$^{-/-}$ recipient (indicated at the top), with using control BALB/c mLN (NFW, nuclease-free water; $n = 5$). **c** A representative sample of Bcl-6 expression in the lymphoma cells injected in *Rag1*$^{-/-}$ recipients (Bcl-6, grey shade overlaid with control labeling (empty histogram with dotted line; $n = 5$)

Discussion

The present paper describes a new high-grade follicular lymphoma type from a BALB/c mouse. Unlike the majority of other mouse lymphoma models, this tumor arose without any previous induction, such as viral or other microbial infection, exposure to chemical carcinogens, or employing genetic manipulation by introducing mutated proto-oncogenes or other regulatory elements [3], therefore its origin is closer to the human conditions. Its restricted intraabdominal expansion via the mesenteric lymphatic vessels embedded in the mesentery may potentially offer a novel animal model for studying

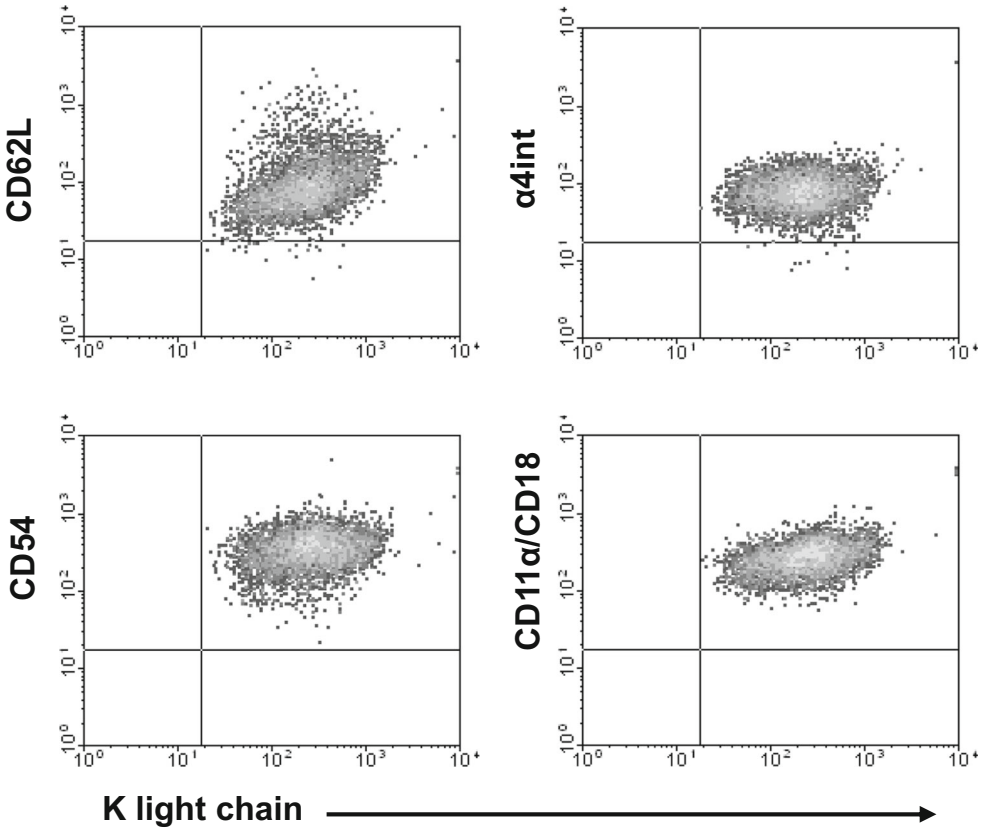

Fig. 5 Adhesion and homing receptor expression by Bc-DLFL.1 lymphoma cells. Lymphoma cells from *Rag1*$^{-/-}$ recipients' mLN were labeled for various adhesion molecules (indicated at the vertical axis) and surface Ig κ-chain together with B220 staining. Density plots depict the expression of adhesion molecule plotted against surface Ig κ-chain of B220^{+} lymphocytes ($n = 7$)

the dissemination of both normal and pathological B cells via the lymphatic circulation.

The lymphoma was identified as germinal center cell derived lymphoma (mixed cell follicular lymphoma) composed of a mixture of centrocytes and centroblasts. Follicular lymphoma is one of the most common types of human lymphomas and is characterized by a nodular pattern containing recognizable follicular structures. This type of lymphoma is composed of centroblasts and centrocytes, the frequency of the previous determines the grade. Low grade follicular lymphomas have an indolent course, while high grade follicular lymphomas overlap with diffuse large B cell lymphoma. Follicular lymphomas in mice rarely show follicular structures; however, the cytology of the lymphoma cells is similar to human cases. When the ratio of centroblasts to centrocytes exceeds 50 %, the case is identified as centroblastic diffuse large B cell lymphoma; however, distinguishing atypical centrocytes from smaller centroblasts is often difficult [2]. While human follicular lymphoma is usually nodal and frequently involves the bone marrow, in mice follicular lymphoma usually involves the spleen with variable enlargement of mLNs and Peyer's patches. In this lymphoma and in subsequent serial transplantations the Peyer's patches were unaffected, whereas mLNs regularly showed robust lymphoma growth.

Flow cytometric analyses established that the lymphoma cells expressed CD19, MHC Class II, B220, supporting that the malignant transformation affected B cells. Furthermore, the expression of surface BcR of IgG2a/κ light chain isotype also indicated mature B-cell origin, unlike the frequent B-cell progenitor tumors observed in mice with conditional Pax5-deletion [11]. The combined phenotypic characterization and IgH V-region rearrangement analysis revealed that, within the B-lineage, the lymphoma cells most likely have originated from a germinal center stage subset, also supported by the presence of Bcl-6 protein. The analysis of IgH V-region rearrangement in both BALB/c and *Rag2*$^{-/-}$ recipients demonstrated identical IgH recombination involving the V_H7183 family only, despite the extensive interspersion with V_HQ52 family segments [15]. The eventual affinity maturation affecting the V-region has not been further explored, but could reveal affinity maturation against an as yet unidentified antigen. Based on its cytological appearance together with the phenotypic analyses, we designate this lymphoma to the high-grade variant of follicular lymphoma, denoted as Bc-DLFL.1.

The restricted distribution of Bc-DLFL.1 cells following intraperitoneal injection raised the issue of preferential migration of lymphoma cells towards spleen and mLN mediated by cell surface adhesion molecules, and also the availability of survival signals promoting lymphoma growth within these lymphoid organs. The fact that the lymphoma cells could successfully be propagated in both BALB/c and *Rag1*$^{-/-}$ recipients indicates that the lymphoma cells do not need fully structured peripheral

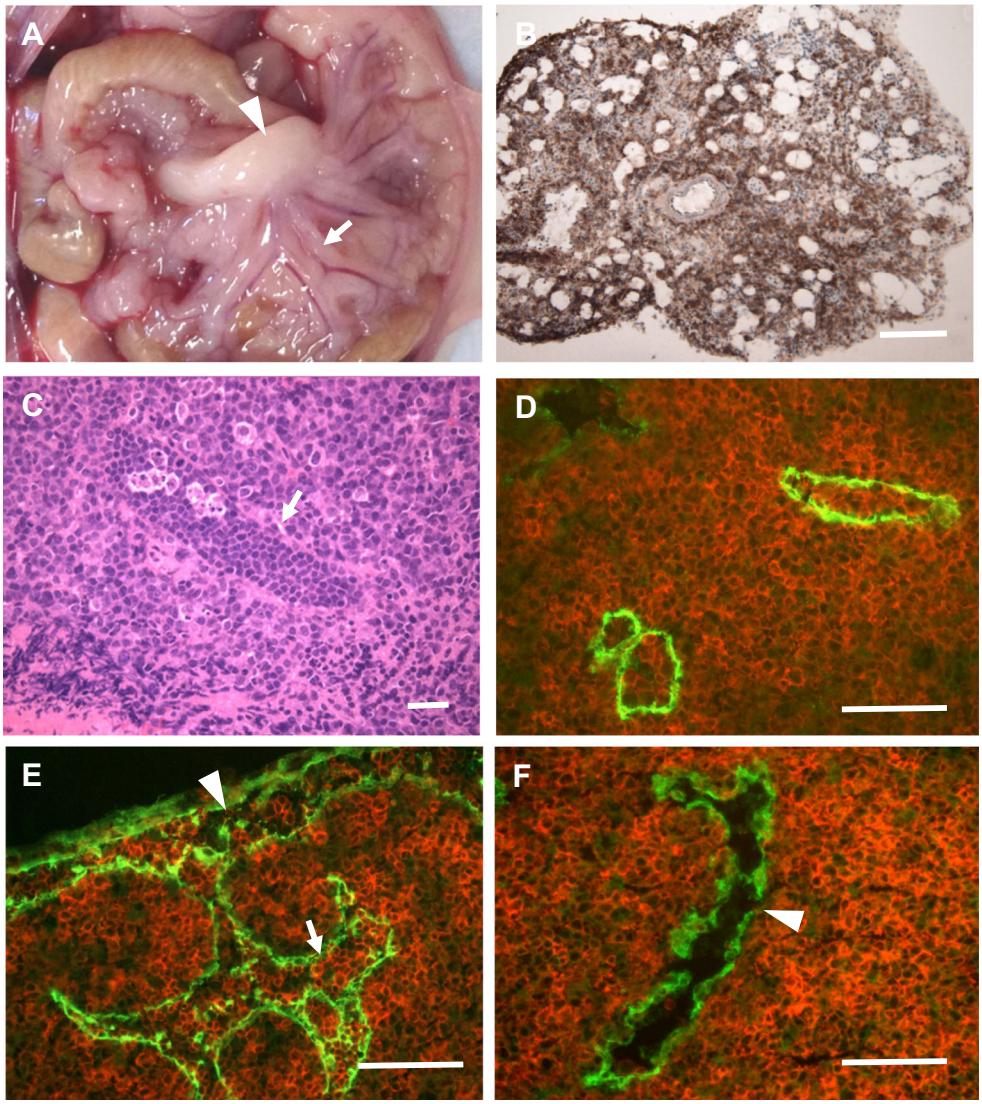

Fig. 6 Mesenteric propagation of Bc-DLFL.1 lymphoma cells involves lymphatic vessels. **a** Perivascular spreading in the mesentery (*arrow*) draining towards the mLN (*arrowhead*) of Bc-DLFL.1 lymphoma cells in BALB/c recipient following ip. injection involves **b** a compact accumulation of B220-positive lymphoma cells (*brown* with *blue* hematoxyline counterstain), also visible in dilated lymphatic vessels (*arrow* in **c**; H&E stain). **d** Dual immunofluorescent staining of mesentery for LYVE-1 (*green*) and B220 (*red*) shows tight clustering both inside and outside the lymphatic capillaries. **e** mLN section stained for B220 (*red*) and LYVE-1 also demonstrates numerous lymphoma cells both in the subcapsular sinus (arrowhead) and the corticomedullary lymphatic sinuses (*arrow*), whereas **f** the PNAd-positive HEVs labeled with MECA-79 mAb (*green*, *arrowhead*) are devoid of lymphoma cells ($n = 5$; scale bars =100 μm)

lymphoid tissues, as $Rag^{-/-}$ recipients lack follicular dendritic cells (FDC), the main stromal constituents in follicles [16], although the Bc-DLFL.1 lymphoma cells express CXCR5 chemokine receptor for the B-cell homeostatic CXCL13 chemokine produced by FDCs [17, 18] (not shown).

Efficient homing to peripheral lymphoid tissues is initiated by specific interaction between recirculating leukocytes and endothelial cell surface adhesion molecules. Of the four adhesion receptors tested we found that, under identical labeling conditions, the expression of ICAM-1 and LFA-1 was higher compared to those of L-selectin and α4 integrin. The combined level of latter two molecules, however, may be sufficient to promote mLN-directed migration, as the high endothelial venules in mLN co-express PNAd and MAdCAM-1 addressins as docking molecules for L-selectin and α4 integrin, respectively, whereas the lower level of L-selectin may reduce the degree of lymphoma homing to pLN where only PNAd acts as homing addressin [19].

Importantly, in addition to the grossly enlarged mLNs, the mesenteric perivascular adipose cuffs also showed an extensive tumor infiltrate. Our findings indicate that, within the adipose-associated vasculature of the mesentery, LYVE-1-positive lymphatic vessels contain large number of lymphoma cells. These lymphatics share numerous phenotypic and transcriptional features with the venous sack-derived lymphatic vessels that drain the skin towards the pLNs; however, their embryonic formation from local mesodermal precursors in the dorsal mesentery is a region-specific process, as it is promoted by the local arteriogenesis with the involvement of CXCR4/CXCL12 interaction [20]. The lymphoma cell-laden mesenteric lymphatics raised the possibility that the lymphoma cells may enter the mLNs via these segments. In the intraperitoneal lymphocyte recirculation under physiological circumstances the main exchange occurs through the milky spots in the omentum [21], but other migratory pathways and locations with distinct integrin requirements and lymphocyte preferences may also be present [22]. The lymphatic

vessels of mesentery are engaged in processing the largest fraction of lymph flow from the gut towards the mLNs [23] and may act as such a draining element. In addition, the mesenteric perivascular fat tissue also harbors aggregates composed of type 2 innate lymphoid cells producing Th2-type cytokines that promote peritoneal B1 B-cell survival [24]. However, the direct entry and subsequent migration of intraperitoneally injected cells (either normal resting lymphocytes or Bc-DLFL.1 lymphoma cells) as first steps of lymphatic propagation require further investigation.

Once traversed into the mesenterial lymphatics, leukocytes may enter the mLNs via the afferent lymphatics. In contrast to the homing via the blood endothelial cells within the high endothelial venules (HEVs), this type of lymphoid cell homing to peripheral lymph nodes (pLNs) has only recently been addressed. According to these findings, skin-derived dendritic cells and also lymphatic-derived T cells require CCR7 and ligand binding to several adhesion proteins (ICAM-1 and VCAM-1) for trans-lymphatic migration. Here the migratory cells are also influenced by the activity of S1P1 receptor in determining entry versus egress through the lymphatics, as defined by the combination of sensitization/desensitization effects of CCL19/CCL21 and S1P gradients [25, 26]. During this process T cells are also exposed to IL7 acting as survival factor [27]. The dissemination of germinal center-derived B- lymphoma cells may be related to the activity of sphingosine-1-phosphate receptor-2 (S1PR2), as mutations affecting S1PR2 or its associated partners Gα12 and Gα13 cause impaired confinement and subsequent dissemination of lymphoma cells [28]. It remains to be determined whether the above adhesion proteins or migratory signalization pathways are affected in the restricted in vivo abdominal propagation of Bc-DLFL.1 cells.

Acknowledgments This work was supported by SROP-4.2.2/B-10/1-2010-0029 and CABCOS II (HUHR/1001/2.1.3/0007) project grant at the University of Pécs. Z K is supported by the Apáczai Csere János Fellowship in the framework of SROP 4.2.4. A/1-11-1-2012-0001 'National Excellence Program' and the postdoctoral research grant of the Faculty of Medicine, University of Pécs. PB is supported by the Hungarian Scientific Research Fund (OTKA K108429), and the research grant IBD-0341 from the Broad Medical Research Program of The Eli and Edythe Broad Foundation. DV and ZK are equal first authors.

Compliance with Ethical Standards

Declaration All applicable international, national, and/or institutional guidelines for the care and use of animals were followed.

References

1. Deshpande AJ, Buske C, Quintanilla-Martinez L, Fend F (2010) In: Dunphy CH (ed) Molecular oncogenesis in Molecular pathology of hematolymphoid diseases. Springer, New York Dordrecht Heidelberg London, pp. 3–21
2. Morse HC 3rd , Anver MR, Fredrickson TN, Haines DC, Harris AW, Harris NL, Jaffe ES, Kogan SC, MacLennan IC, Pattengale PK, Ward JM (2002) Hematopathology subcommittee of the mouse models of human cancers consortium. Bethesda Proposals for Classification of Lymphoid Neoplasms in Mice Blood 100:246–258.
3. Donnou S, Galand C, Touitou V, Sautès-Fridman C, Fabry Z, Fisson S (2012) Murine models of B-cell lymphomas: promising tools for designing cancer therapies. Adv Hematol 2012:701704. doi:10.1155/2012/701704
4. Kovalchuk AL, Qi CF, Torrey TA, Taddesse-Heath L, Feigenbaum L, Park SS, Gerbitz A, Klobeck G, Hoertnagel K, Polack A, Bornkamm GW, Janz S, Morse HC 3rd (2000) Burkitt lymphoma in the mouse. J Exp Med 192:1183–1190
5. Strasser A, Harris AW, Vaux DL, Webb E, Bath ML, Adams JM, Cory S (1990) Abnormalities of the immune system induced by dysregulated bcl-2 expression in transgenic mice. Curr Top Microbiol Immunol 166:175–181
6. Egle A, Harris AW, Bath ML, O'Reilly L, Cory S (2004) VavP-Bcl2 transgenic mice develop follicular lymphoma preceded by germinal center hyperplasia. Blood 103:2276–2283
7. Balogh P, Lábadi P (2011) Structural evolution of the spleen in man and mouse in developmental biology of peripheral lymphoid organs Ed. P. Balogh springer-verlag. Berlin Heidelberg 2011:121–142
8. Kim HJ, Kammertoens T, Janke M, Schmetzer O, Qin Z, Berek C, Blankenstein T (2004) Establishment of early lymphoid organ infrastructure in transplanted tumors mediated by local production of lymphotoxin alpha and in the combined absence of functional B and T cells. J Immunol 172:4037–4047
9. Höpken UE, Rehm A (2012) Homeostatic chemokines guide lymphoma cells to tumor growth-promoting niches within secondary lymphoid organs. J Mol Med (Berl) 90:1237–1245
10. Mombaerts P, Iacomini J, Johnson RS, Herrup K, Tonegawa S, Papaioannou VE (1992) RAG-1-deficient mice have no mature B and T lymphocytes. Cell 68:869–877
11. Cobaleda C, Jochum W, Busslinger M (2007) Conversion of mature B cells into T cells by dedifferentiation to uncommitted progenitors. Nature 449:473–477
12. Frith CG, Wiley LD (1981) Morphologic classification and correlation of incidence of hyperplastic and neoplastic hematopoietic lesions in mice with age. J Gerontol 36:534–545
13. Bunting KL, Melnick AM (2013) New effector functions and regulatory mechanisms of BCL6 in normal and malignant lymphocytes. Curr Opin Immunol 25:339–346
14. Basso K, Dalla-Favera R (2012) Roles of BCL6 in normal and transformed germinal center B cells. Immunol Rev 247:172–183
15. Johnston CM, Wood AL, Bolland DJ, Corcoran AE (2006) Complete sequence assembly and characterization of the C57BL/6 mouse Ig heavy chain V region. J Immunol 176:4221–4234
16. Fu YX, Huang G, Wang Y, Chaplin DD (1998) B lymphocytes induce the formation of follicular dendritic cell clusters in a lymphotoxin alpha-dependent fashion. J Exp Med 187:1009–1018
17. Förster R, Mattis AE, Kremmer E, Wolf E, Brem G, Lipp M (1996) A putative chemokine receptor, BLR1, directs B cell migration to defined lymphoid organs and specific anatomic compartments of the spleen. Cell 87:1037–1047
18. Ansel KM, Ngo VN, Hyman PL, Luther SA, Förster R, Sedgwick JD, Browning JL, Lipp M, Cyster JG (2000) A chemokine-driven positive feedback loop organizes lymphoid follicles. Nature 406:309–314
19. Rosen SD (2004) Ligands for L-selectin: homing, inflammation, and beyond. Annu Rev Immunol 22:129–156
20. Mahadevan A, Welsh IC, Sivakumar A, Gludish DW, Shilvock AR, Noden DM, Huss D, Lansford R, Kurpios NA (2014) The left-right Pitx2 pathway drives organ-specific arterial and lymphatic development in the intestine. Dev Cell 31:690–706

21. Ansel KM, Harris RB, Cyster JG (2002) CXCL13 is required for B1 cell homing, natural antibody production, and body cavity immunity. Immunity 16:67–76
22. Berberich S, Dähne S, Schippers A, Peters T, Müller W, Kremmer E, Förster R, Pabst O (2008) Differential molecular and anatomical basis for B cell migration into the peritoneal cavity and omental milky spots. J Immunol 180:2196–2203
23. Gashev AA (2010) Basic mechanisms controlling lymph transport in the mesenteric lymphatic net. Ann N Y Acad Sci 1207(Suppl 1): E16–E20
24. Moro K, Yamada T, Tanabe M, Takeuchi T, Ikawa T, Kawamoto H, Furusawa J, Ohtani M, Fujii H, Koyasu S (2010) Innate production of T(H)2 cytokines by adipose tissue-associated c-kit(+)Sca-1(+) lymphoid cells. Nature 463:540–544
25. Braun A, Worbs T, Moschovakis GL, Halle S, Hoffmann K, Bölter J, Münk A, Förster R (2011) Afferent lymph-derived T cells and DCs use different chemokine receptor CCR7-dependent routes for entry into the lymph node and intranodal migration. Nat Immunol 12:879–887
26. Förster R, Braun A, Worbs T (2012) Lymph node homing of T cells and dendritic cells via afferent lymphatics. Trends Immunol 33: 271–280
27. Miller CN, Hartigan-O'Connor DJ, Lee MS, Laidlaw G, Cornelissen IP, Matloubian M, Coughlin SR, McDonald DM, McCune JM (2013) IL-7 production in murine lymphatic endothelial cells and induction in the setting of peripheral lymphopenia. Int Immunol 25:471–483
28. Muppidi JR, Schmitz R, Green JA, Xiao W, Larsen AB, Braun SE, An J, Xu Y, Rosenwald A, Ott G, Gascoyne RD, Rimsza LM, Campo E, Jaffe ES, Delabie J, Smeland EB, Braziel RM, Tubbs RR, Cook JR, Weisenburger DD, Chan WC, Vaidehi N, Staudt LM, Cyster JG (2014) Loss of signalling via Gα13 in germinal Centre B-cell-derived lymphoma. Nature 516:254–258